Available online at www.sciencedirect.com

ScienceDirect

Procedia Materials Science 3 (2014) 1135 – 1142

Procedia Materials Science

www.elsevier.com/locate/procedia

20th European Conference on Fracture (ECF20)

Simulation of deformation-induced martensite formation and its influence on the resonant behavior in the very high cycle fatigue (VHCF) regime

P.-M. Hilgendorff[a,*], A. Grigorescu[b], M. Zimmermann[c], C.-P. Fritzen[a], H.-J. Christ[b]

[a]*Institut für Mechanik und Regelungstechnik - Mechatronik, Universität Siegen, 57068 Siegen, Germany*
[b]*Institut für Werkstofftechnik, Universität Siegen, 57068 Siegen, Germany*
[c]*Institut für Werkstoffwissenschaft, Technische Universität Dresden, 01062 Dresden, Germany*

Abstract

The exploration of fatigue mechanisms in the VHCF regime is gaining importance since many components have to withstand a very high number of loading cycles due to high frequency or long product life. In this regime, particular attention is paid to the period of fatigue crack initiation and thus the localization of plastic deformation. The resonant behavior of a metastable austenitic stainless steel (AISI304) is studied experimentally in the VHCF regime and shows a distinct transient characteristic. The major contribution of this work is to obtain a physically-based understanding of this characteristic by modeling the underlying microstructural mechanisms and their influence on the resonant behavior. Microscopic examinations indicate that AISI304 undergoes deformation-induced martensite formation starting mostly at intersecting shear bands during fatigue. Therefore, a microstructural shear band model [Hilgendorff et al. (2013)] is extended regarding the mechanism of deformation-induced martensite formation. The model accounts for the microstructural mechanisms occurring in shear bands as documented by experimental results, and nucleation of martensite is assumed to occur at intersecting shear bands following the Olsen-Cohen nucleation model (1972) in combination with the Bogers-Burgers mechanism (1964). The simulation model is numerically solved using the two-dimensional (2-D) boundary element method. By using this method, a 2-D microstructure can be modeled considering grain orientations as well as individual anisotropic elastic properties in each grain. The resonant behavior is characterized by evaluating the force-displacement hysteresis loop. Results show that plastic deformation in shear bands and deformation-induced martensite formation have a major impact on the resonant behavior in the very high cycle fatigue (VHCF) regime.

Selection and peer-review under responsibility of the Norwegian University of Science and Technology (NTNU), Department of Structural Engineering

Keywords: Simulation, deformation-induced martensite, resonant behavior, boundary element method, very high cycle fatigue

Selection and peer-review under responsibility of the Norwegian University of Science and Technology (NTNU), Department of Structural Engineering
doi:10.1016/j.mspro.2014.06.185

1. Introduction

In recent years the number of applications in which structural components are cyclically loaded up to a very high number of loading cycles has risen continually due to the need for increased economic efficiency. In turn, to guarantee the safety of human, machine and environment the exploration of very high cycle fatigue (VHCF) damage mechanisms and the characterization of fatigue life are of particular importance.

In the VHCF regime the overall fatigue life is predominantly determined by the period of fatigue crack initiation and thus the localization of plastic deformation. The metastable austenitic stainless steel (AISI304, initially pure austenitic condition) that is investigated in this study shows localization of plastic deformation in shear bands and, furthermore, undergoes a deformation-induced phase transformation from the ductile γ-austenite into the harder α'-martensite phase. In order to investigate the effect of these two respective microstructural changes on the cyclic deformation behavior, this study focuses on the correlation between the monitored resonant behavior of specimens and the fatigue behavior. On the one hand modern resonance-testing-machines allow a convenient and very accurate measuring of the resonant behavior in terms of the resonant frequency and on the other hand the knowledge of the impact of microstructural changes related to damage mechanisms on the resonant behavior will be highly beneficial for investigations in the field of structural health monitoring (SHM).

In the following paragraphs at first the results of experimental examinations in terms of the transient characteristic of the resonant behavior and microscopic observations are given. Then, for assigning the plastic deformation in shear bands and phase transformation to the transient characteristic a simulation model is presented in which the mechanisms of shear band formation and deformation-induced martensitic transformation are proposed. Furthermore, as a method of numerical simulation the boundary element method (BEM) is specified that is well suited to investigate the effect of the suggested simulation model. After presenting a procedure to determine the resonant behavior based on the results from microstructural simulations, the influence of localization of plastic deformation in shear bands and deformation-induced martensite formation on the resonant behavior is investigated regarding the morphology of a real microstructure.

Nomenclature

a_{fcc}	lattice constant of face centered cubic structure
c_{ij}	numerical parameter that equals 0.5 when Γ_b is smooth
f_0, f_{res}	undamped and damped resonant frequency
n_α	outward unit normal vector
p_i	tractions
$u_i, \Delta u_i$	displacements and relative displacements
C_{ijkl}	elasticity tensor
$\boldsymbol{T}$	Burgers vector of a Shockley partial dislocation
η_{res}	resonant frequency ratio
$\sigma_{i\alpha}$	stresses
τ	shear stress
Γ_b, Γ_s	external boundary and slip line face
$\boldsymbol{d}^*(\boldsymbol{x},\boldsymbol{y})$, $\boldsymbol{p}^*(\boldsymbol{x},\boldsymbol{y})$, $\boldsymbol{u}^*(\boldsymbol{x},\boldsymbol{y})$, $\boldsymbol{s}^*(\boldsymbol{x},\boldsymbol{y})$	fundamental solutions of the boundary element method

2. Experimental characterization

The resonant behavior of a metastable austenitic stainless steel (AISI304) is studied experimentally by means of a resonance-testing-machine, which readjusts the excitation resonant frequency during testing. Fig. 1a shows two separate curves for the testing frequencies over cycles. The lower curve indicates the testing frequencies measured at a stress amplitude in the range of the VHCF strength (240 MPa), representing the damped resonant frequency f_{res} of the specimen-machine system. It describes a distinct transient characteristic over cyclic loading consisting of cyclic softening (decrease of f_{res}) followed by cyclic hardening (increase of f_{res}). In contrast, the upper curve indicates the testing frequencies at a stress amplitude of 50 MPa measured at distinct fatigue stages that were reached due to

testing at 240 MPa. These frequencies represent the resonant frequency f_0 of the sample without the damping effect of plastic deformation. Fig. 1b shows a TEM micrograph of α'-martensite nuclei (dark areas) at intersecting shear bands formed in metastable austenitic stainless steel fatigued under VHCF condition. In the upper right of the micrograph the assumed directions of surface slip markings of participating shear bands are indicated.

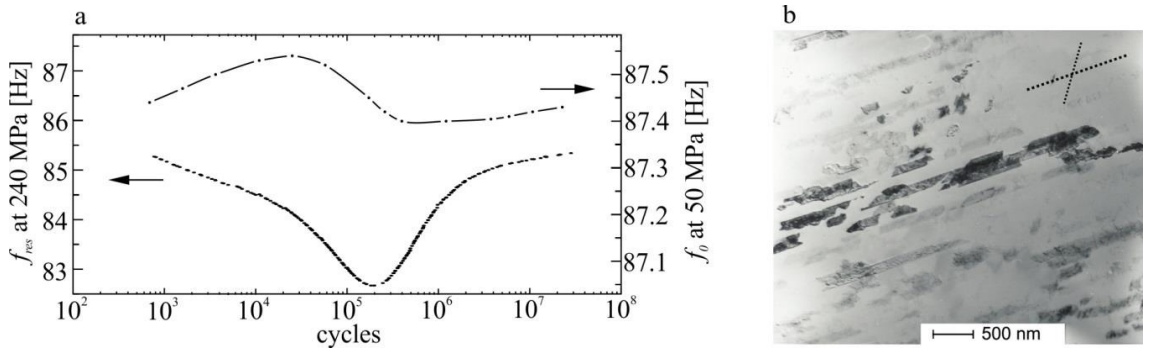

Fig. 1. (a) damped f_{res} and undamped f_0 resonant frequency during fatigue; (b) TEM micrograph of generated α'-martensite.

3. Simulation model

In the present study the simulation model focuses on plastic deformation in shear bands on the one hand and on deformation-induced martensite formation on the other hand as they are the predominant microstructural processes in the originally fully austenitic condition of the metastable austenitic stainless steel AISI304 during cyclic deformation in the VHCF regime [Müller-Bollenhagen 2010].

The localization of cyclic plastic deformation in shear bands will be considered by certain mechanisms which were proposed in [Hilgendorff et al. (2013)] and are briefly summarized as follows. Formation of a shear band is assumed to occur at sites of shear stress concentration once a critical resolved shear stress in the most critical slip system is exceeded. The sliding distribution along the shear band arises from the theory of dislocation pile-ups at grain boundaries and the irreversible shear character is represented as the shear band is approximated by two closely located layers and a special procedure is applied to accumulate the irreversible fraction of cyclic shear. The proposed model is successfully applied on a mesoscopic scale by numerically solving it with the boundary element method.

Microscopic examinations indicate and there is also good agreement in the literature [Bayerlein et al. 1989] that apart from a pronounced surface roughening by shear bands the material (AISI304) also undergoes deformation-induced martensitic transformation (from γ to α') at intersecting shear bands in the VHCF regime. These observations are used in the present study to develop a martensitic transformation model. The model proposed in this study is based on three pillars: the crystallographic orientation relationship between austenite and generated martensite (1), the mechanism of martensite nucleation and growth (2) and the shape deformation induced by transformation (3). They are described as follows.

It has been reported that the orientation of the α'-martensite (body centered cubic, bcc) to the γ-austenite (face centered cubic, fcc) phase resembles the Kurdjumov-Sachs (K-S) relationship [Christ et al. 2009]. As the K-S relationship can be described mathematically as a rotation matrix, the elastic and the plastic anisotropic properties of generated martensite nuclei can be specified by rotation of the elasticity tensor C_{ijkl} and the slip systems of the bcc structure, respectively.

The mechanism of martensite nucleation and growth proposed in this study incorporates the effect of the actual atomistic paths during transformation and builds on a model proposed by Roth et al. [Roth 2011]. It is based on the Bogers-Burgers (1964) double shear mechanism that describes the transformation from fcc to bcc and is supplemented by suggestions of Olsen and Cohen (1972). According to the Bogers-Burgers model, a bcc structure can be generated from fcc structure by two shears: a first shear that involves one-third of the Burgers vector of a

Shockley partial dislocation ($\boldsymbol{T}=a_{\mathrm{fcc}}/6$ <112>) along successive $\{111\}_{\mathrm{fcc}}$ planes and a second shear that involves $\boldsymbol{T}/2$ along other successive $\{111\}_{\mathrm{fcc}}$ planes. Olsen and Cohen extended the model regarding plausible dislocation motions and proclaim that the Bogers-Burgers hypothesis is most likely to be valid within the intersected volume of two shear bands in which atoms can attain true bcc positions. Hence, the hypothesis applies to the metastable austenitic stainless steel studied with its intersecting shear bands as shown in Fig. 1b. In addition, results of simulation of damage accumulation in shear bands (with the shear band model enabled) indicate that in a real simulated 2-D microstructure multiple slip, and thereby, interactions of shear bands arise. Therefore, the previously described mechanism in combination with the shear band model is used to identify potential sites of martensite nucleation on the one hand and to determine the size of generated martensite domains on the other hand depending on the direction and amount of shear deformation in participating shear bands.

Apart from a shear component both Bogers-Burgers shears entail a dilatation component normal to the shear planes because atoms must ride up to a saddle-point position between the initial and final states. The shape deformation of each Bogers-Burgers shear can be accurately described as an invariant-plane strain (IPS), which consists of a uniaxial dilatation and a simple shear ([Yang 2010], [Christian 2002]) and can be combined to one IPS by simple matrix multiplication. In view of continuum mechanics the IPS is a kind of deformation gradient tensor that allows to calculate the corresponding transformation strains ε^{p} assuming small deformation theory. Thus, the shape deformation induced by transformation depending on individual shear combination is adequately described.

After the mechanisms of shear band formation and deformation-induced martensitic transformation are defined in the simulation model, in the following the numerical method is presented.

4. Numerical method

The 2-D boundary element method is well suited to investigate the effect of the proposed simulation model. The formulation used in this study combines the traditional displacement BEM as well as the displacement discontinuity BEM [Kübbeler 2011] and is newly enhanced in terms of initial strains which may be defined as transformation strains ε^{p}. By doing so, sliding displacements can be directly evaluated in shear bands and austenite grains as well as generated martensite domains with its individual mechanical properties and shape deformation can be considered.

The procedure is based on two boundary integral equations: the displacement boundary integral equation, which is applied on the external boundary Γ_{b} (grain and phase boundaries), and the stress boundary integral equation, which is used on the slip line faces Γ_{s} (shear bands). On the external boundary Γ_{b} displacements and tractions with components u_i and p_i are prescribed, while relative displacements Δu_i and stresses $\sigma_{i\alpha}$ are considered on one face Γ_{s} of the slip line. The displacement integral equation for a solid containing a shear line can be written as:

$$c_{ij}u_j(\boldsymbol{x}) = \int_{\Gamma_b}\left[u_{ij}^*(\boldsymbol{x},\boldsymbol{y})p_i(\boldsymbol{y}) - p_{ij}^*(\boldsymbol{x},\boldsymbol{y})u_i(\boldsymbol{y}) + u_{ij}^*(\boldsymbol{x},\boldsymbol{y})C_{i\alpha s\lambda}n_\alpha\varepsilon_{s\lambda}^{\mathrm{p}}\right]d\Gamma_y + \int_{\Gamma_s} p_{ij}^*(\boldsymbol{x},\boldsymbol{y})\Delta u_i(\boldsymbol{y})d\Gamma_y,\ \boldsymbol{x}\in\Gamma_b \qquad (1)$$

where c_{ij} equals 0.5 when Γ_b is smooth and $C_{i\alpha s\lambda}$ and n_α are the elasticity tensor and outward unit normal vector, respectively. Vector $\boldsymbol{x}$ denotes the positions, where displacements are determined, and $\boldsymbol{y}$ denotes the integration points on the boundaries Γ_b and Γ_{s}. $u_{ij}^*(\boldsymbol{x},\boldsymbol{y})$ and $p_{ij}^*(\boldsymbol{x},\boldsymbol{y})$ are the displacement and the traction fundamental solutions and are given in [Hilgendorff et al. (2013)]. The stress boundary integral equation is obtained by substituting equation (1) into Hooke's law:

$$\sigma_{j\gamma}(\boldsymbol{x}) = \int_{\Gamma_b}\left[d_{ij\gamma}^*(\boldsymbol{x},\boldsymbol{y})\,p_i - s_{ij\gamma}^*(\boldsymbol{x},\boldsymbol{y})u_i + C_{j\gamma p\delta}u_{ip,\delta}^*(\boldsymbol{x},\boldsymbol{y})C_{i\alpha s\lambda}n_\alpha\varepsilon_{s\lambda}^{\mathrm{p}}\right]d\Gamma + \int_{\Gamma_s} s_{ij\gamma}^*(\boldsymbol{x},\boldsymbol{y})\Delta u_i(\boldsymbol{y})d\Gamma - C_{j\gamma p\delta}\varepsilon_{p\delta}^{\mathrm{p}},\ \boldsymbol{x}\in\Gamma_s \quad (2)$$

where $d_{ij\gamma}^*(\boldsymbol{x},\boldsymbol{y})$ and $s_{ij\gamma}^*(\boldsymbol{x},\boldsymbol{y})$ are the stress and the higher-order stress fundamental solutions [Hilgendorff et al. (2013)].

Previously, the BEM was derived for a single homogeneous solid. In case of microstructural modeling it is advisable to consider several grains with individual anisotropic elastic properties. Therefore, a substructure

technique is applied which enables coupling of individual homogeneous structures by use of continuity condition [Kübbeler 2011]. Finally, a 2-D microstructure consisting of austenite grains and martensite domains with individual anisotropic elastic properties can be represented.

5. Resonant behavior

A prediction of the effect of microstructural changes due to localization of plastic deformation in shear bands and deformation-induced martensite formation on the resonant behavior requires a procedure to describe the resonant behavior based on the results from the microstructural simulations. With the use of both the viscous and the hysteretic damping model [Gaul 1985] an equivalent damping ratio D and the resonant frequency ratio η_{res} as a describing parameter for the resonant behavior can be identified. η_{res} is basically defined as the ratio of resonant frequency of the damped system (f_{res}) and that of the undamped system (f_0). By means of energy loss per cycle ΔW, stiffness k of the specimen and displacement amplitude $\hat{x}$ of the force displacement hysteresis loop the ratio η_{res} is given by:

$$\eta_{res} = \sqrt{1 - \frac{\Delta W^2}{2\pi^2 \cdot k^2 \cdot \hat{x}^4}} \,. \tag{3}$$

ΔW, k and $\hat{x}$ can be taken from the hysteresis loop, which is calculated during simulation. η_{res} can also be evaluated by using the experimental results depicted in Fig. 1a. Thus, the ratio η_{res} is applicable to compare the results from experiments with those from simulations.

6. Simulation of localized cyclic deformation and phase transformation

The implementation of the simulation model into the BEM allows for simulation of the effect of the suggested simulation model on the resonant behavior and damage relevant parameters such as shear stresses. The investigation was carried out on the basis of the real microstructure of a metastable austenitic stainless steel characterized by means of scanning electron microscopy (SEM) in combination with the electron backscattered diffraction (EBSD)-technique and the orientation imaging microscopy (OIM) analysis.

The SEM image, EBSD map and phase map of the observed microstructure are shown in Fig. 2a, 2b and 2c, respectively. In addition to grain boundaries, the SEM image also highlights markings of emerging slip bands at the surface after cyclic loading. The EBSD map in Fig. 2b with related stereographic triangle indicates the crystallographic orientation of each grain and the phase map points out sites of generated α'-martensite phases (green areas).

Fig. 3 shows contours of simulated shear stresses in most critical slip systems in the microstructure for two different simulations. Figs. 3a and 3b illustrate the results for the first and third simulated loading cycle when both the shear band and the martensite model are enabled. In contrast, Fig. 3c shows the contour for the third loading cycle when only the shear band model is enabled while martensite formation is not allowed. Contours were chosen in each case at the maximum external loading of 240 MPa (here: stresses are introduced as boundary condition to the observed microstructure) and evolved shear bands are emphasized by white dotted lines. Due to high computational effort, damage modeling was confined to one grain labeled A in Fig. 3a. It should be noticed that one cycle in the simulation represents the microstructural damage evolution resulting from many cycles in the experiment. This was achieved by adapting the influence of cyclic slip irreversibility and by similarly increasing the size of generated α'-martensite per cycle.

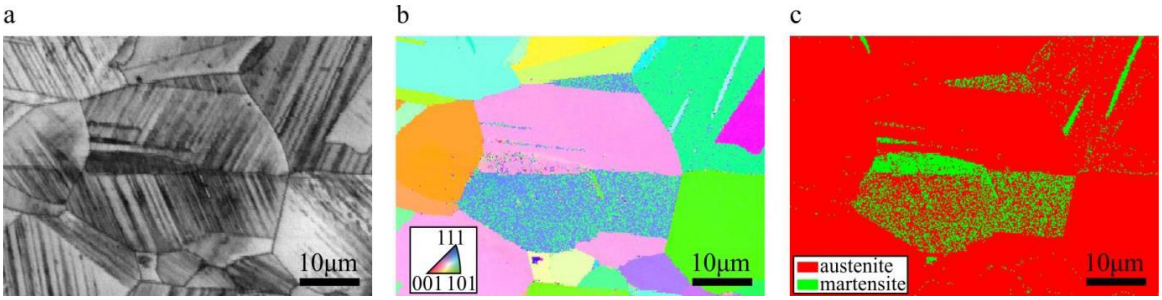

Fig. 2. (a) SEM image; (b) EBSD map; (c) phase map of the measured zone of surface grains (stress amplitude 240 MPa, cycles: 10^7).

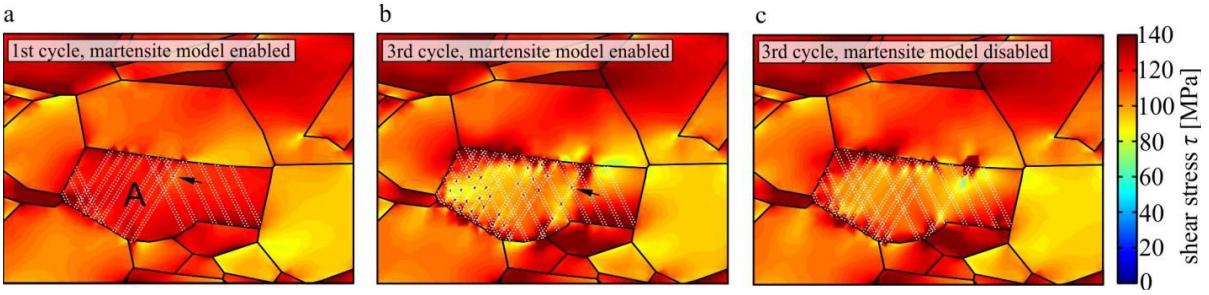

Fig. 3. (a) Contours of simulated maximum shear stresses in most critical slip systems in the 1st (a) and 3rd (b) loading cycle when both shear band and martensite model are enabled (martensite formation is indicated by arrows) and in the 3rd loading cycle (c) when only the shear band model is enabled (stress amplitude 240 MPa).

The small dark dots indicated by small arrows in Figs. 3a and 3b represent very localized stress peaks where α'-martensite was generated at intersecting shear bands. Thus, the simulation model of the observed grain is able to mimic multiple activation of slip systems leading to deformation-induced martensite formation within the grain as is confirmed by experimental observations (Fig. 2c). Due to gradual increase of plastic deformation in shear bands the number and size of generated martensite embryos are growing with increasing number of simulated loading cycles (compare Figs. 3a and 3b). The comparison of the contour plots depicted in Figs. 3b and 3c shows that through the presence of the martensite phase the maximum shear stresses τ are slightly reduced within the observed grain. This effect is attributed to the shape deformation that is introduced by generated martensite domains (see simulation model).

In order to investigate the effect of the simulated microstructural changes on the resonant behavior, the force-displacement hysteresis loop is evaluated for each cycle of simulation and by using Eq. (3) the resonant frequency ratio η_{res} is determined. Fig. 4 shows the qualitative comparison of resonant frequency ratio η_{res} from experiment and two simulations, including one with and one without consideration of martensite modelling. Different assigning of scales for simulation (red) and experiment (black) demonstrate the qualitative manner of this comparison. A decrease of η_{res} relates to cyclic softening and an increase to cyclic hardening.

At present, simulations with consideration of deformation-induced α'-martensite formation and growth have not progressed beyond 4 simulated loading cycles. However, the results in Fig. 4 show that an experimentally observed cyclic softening at the beginning of fatigue (decrease of η_{res}) arise from simulations in both cases, when the martensite model is enabled and disabled. The comparison of the two simulated curves further indicates that martensite formation and growth lead to a weaker softening. Thus, it can be concluded that the experimental confirmed pronounced cyclic softening is mainly determined by the localization of plastic deformation in shear bands whilst the influence of martensite is of secondary importance at this stage of fatigue. Fig. 4 also demonstrates that plastic deformation in shear bands leads to a subsequent cyclic hardening. The investigation of the influence of deformation-induced martensite formation on the period of cyclic hardening will be the subject of future work.

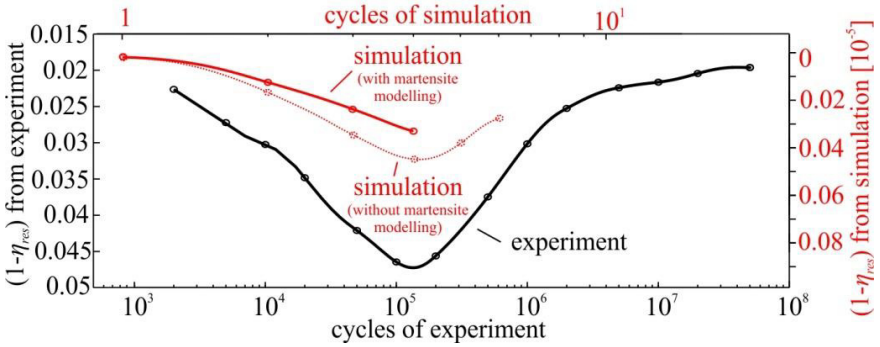

Fig. 4. Qualitative comparison of resonant frequency ratio η_{res} from simulations (with and without martensite modelling) and experiment.

7. Conclusion

In this study a microstructural shear band model [Hilgendorff et al. (2013)] is extended regarding the mechanisms of deformation-induced α'-martensitic transformation. The elastic and plastic anisotropy of generated martensite is defined by assuming the orientation relationship of Kurdjumov-Sachs. The mechanism of martensite nucleation and growth proposed in this study is based on the Bogers-Burgers (1964) double shear mechanism that relates to the transformation from fcc to bcc lattice and is supplemented by suggestions of Olsen and Cohen (1972). Since both Bogers-Burgers shears can be accurately described as invariant-plane strains the transformation strains ε^p due to shape deformation can be derived. The simulation model is implemented into the 2-D boundary element method, so that the influence of localization of plastic deformation in shear bands and deformation-induced martensite formation can be investigated by conducting simulations in a real simulated 2-D microstructure. It turns out in simulations that the shear stresses in most critical slip systems around generated martensite nuclei are slightly reduced due to introduced shape deformation. Sites of originated martensite nuclei are consistent with those observed in the experiments. The resonant behavior is characterized by the resonant frequency ratio η_{res} that can be evaluated from experimental results and simulated force-displacement hysteresis loops. The qualitative comparison of η_{res} from simulation and experiment shows that cyclic softening in the transient regime is mainly determined by damage accumulation in shear bands. It becomes apparent that the deformation-induced α'-martensite formation has a lower effect on the resonant behavior in the period of cyclic softening. Future investigations will concentrate on the effect of martensite during the further course of fatigue in which for instance the experimentally observed formation of martensite needles requires closer examination.

Acknowledgements

The authors gratefully acknowledge financial support of this study by Deutsche Forschungsgemeinschaft (DFG) in the framework of the priority program Life$^{\infty}$ (SPP 1466).

References

Bayerlein, M., Christ, H.-J., Mughrabi, H., 1989, Plasticity-induced martensitic transformation during cyclic deformation of AISI 304L stainless steel. Materials Science and Engineering A, 114, L11-L16.

Bogers, A. J., Burgers, W. G., 1964. Partial dislocations on the {110} planes in the b.c.c. lattice and the transition of the f.c.c. into the b.c.c. lattice. Acta Metallurgica, 12, 255-261.

Christ, H.-J., Krupp U., Mueller-Bollenhagen, C., Roth, I., Zimmermann, M., 2009, Effect of Deformation-Induced Martensite on the Fatigue Behavior of Metastable Austenitic Stainless Steels. 12th International Conference on Fracture, Ottawa, Canada, paper#T12.016.

Christian, J.W., 2002, The theory of transformations in metals and alloys. Pergamon, Oxford.

Gaul, L., Bohlen, S., Kempfle, S., 1985, Transient and Forced Oscillations of Systems with Constant Hysteretic Damping. Mechanics Research Communications, 12, 187-201.

Hilgendorff, P.-M., Grigorescu, A., Zimmermann, M., Fritzen, C.-P., Christ, H.-J., 2013. Simulation of irreversible damage accumulation in the very high cycle fatigue (VHCF) regime using the boundary element method. Materials Science and Engineering A, 575, 169-176.

Kübbeler, M., Roth, I., Krupp, U., Fritzen, C.-P., Christ, H.-J., 2011, Simulation of stage I-crack growth using a hybrid boundary element technique. Engineering Fracture Mechanics, 78, 462-468.

Müller-Bollenhagen, C., Zimmermann, M., Christ, H.-J., 2010, Adjusting the very high cycle fatigue properties of a metastable austenitic stainless steel by means of the martensite content. Procedia Engineering, 2, 1663-1672.

Olsen, G. B., Cohen, M., 1972. A mechanism for the strain-induced nucleation of martensitic transformations. Journal of Less-Common Metals, 28, 107-118.

Roth, I., 2011. Untersuchungen zum Ausbreitungsverhalten mikrostrukturell kurzer Ermüdungsrisse in metastabilem austenitischen Edelstahl, Dissertation, Universität Siegen, Siegen, Germany.

Yang, J.B. Yang, Z.G., Nagaic, Y., Hasegawaa, M., 2010, A crystallographic model of fcc/bcc martensitic nucleation and growth. Acta Materialia, 58 (5), 1599-1606.